J|A|C|S
ARTICLES
Published on Web 03/21/2006

Surface-Rolling Molecules

Yasuhiro Shirai,[§] Andrew J. Osgood,[†] Yuming Zhao,[§] Yuxing Yao,[§] Lionel Saudan,[§] Hanbiao Yang,[§] Chiu Yu-Hung,[§] Lawrence B. Alemany,[§] Takashi Sasaki,[§] Jean-François Morin,[§] Jason M. Guerrero,[§] Kevin F. Kelly,*[,†] and James M. Tour*[,§]

Contribution from the Departments of Chemistry, Mechanical Engineering and Materials Science, and Smalley Institute for Nanoscale Science and Technology, and Department of Electrical and Computer Engineering and Rice Quantum Institute, Rice University, 6100 Main Street, Houston, Texas 77005

Received December 15, 2005; E-mail: kkelly@rice.edu; tour@rice.edu

Abstract: Design, syntheses, and testing of new, fullerene-wheeled single molecular nanomachines, namely, nanocars and nanotrucks, are presented. These nanovehicles are composed of three basic components that include spherical fullerene wheels, freely rotating alkynyl axles, and a molecular chassis. The use of spherical wheels based on C_{60} and freely rotating axles based on alkynes permits directed nanoscale rolling of the molecular structure on gold surfaces. The rolling motion observed by STM resembles the same motion performed by macroscopic entities in which rolling occurs perpendicular to the axles. A new synthesis methodology, in situ ethynylation of fullerenes, was developed for the realization of the fullerene-wheeled molecular machines. Four generations of the fullerene-wheeled structures were developed, and the latest fourth generation nanocar, **3b**, along with three-wheeled triangular compounds, **4a** and **4b**, provided definitive evidence for fullerene-based wheel-like rolling motion, not stick-slip or sliding translation. The studies here underscore the ability to control directionality of motion in molecular-sized nanostructures through precise molecular design and synthesis.

Introduction

The current trend in the physical and biological sciences is the continued miniaturization of machinery from the macroscopic to the microscopic world given that our current scientific, medical, and technological disciplines will increasingly rely on the ability to control the transport of materials, transmission of power, and transfer of information at the microscopic level.[1] The ultimate goal is to build machines at the nanoscopic level from individual atoms.[2] However, this bottom-up approach poses a critical question of how to construct and control the molecular-sized machines. Building such a diminutive machine is no longer a matter of scaling down a macroscopic cousin.[3] The manipulation of nanomachines requires control of the motion and performance at the molecular level.[3−5] From the chemical perspective, the synthesis of various functional molecules as molecular-sized machines might provide insight regarding biomolecular machines[6] and new challenges on the construction and control of miniaturized machines[7] on an unprecedented level. Directed by this objective, and with the hope of directing future bottom-up fabrication through bulk external stimuli, such as electric fields, on nanometer-sized transporters, we have designed and synthesized a class of single molecular vehicles, namely, nanotrucks and nanocars, and sought to study controlled molecular motion on surfaces through the rational design of the surface-capable molecular structures (Figure 1). We report here the synthetic details related to the preparation of these nanomachines, while summarizing the initial imaging and fullerene-based wheel-like rolling motions, as opposed to the more common stick-slip or sliding[8] translation.

At the outset, a definition of terms is helpful since we are defining names of single-molecule entities by analogy to the macroscopic view of vehicles, namely, cars and trucks. As with any analogy, there are similarities and dissimilarities between

[§] Departments of Chemistry, Mechanical Engineering and Materials Science.

[†] Department of Electrical and Computer Engineering.

(1) (a) Timp, G. L. *Nanotechnology*; AIP Press/Springer: New York, 1999. (b) *Nanoelectronics and Information Technology: Advanced Electronic Materials and Novel Devices Information Technology*; Waser, R., Ed.; Wiley-VCH: Weinheim, Germany, 2003.
(2) Feynman, R. P. *Engineering and Science (California Institute of Technology)* **1960**, *23*, 22−36.
(3) (a) Musser, G. *Sci. Am.* **1999**, *280*, 24. (b) Drexler, K. E. *Nanosystems: Molecular Machinery, Manufacturing, and Computation*; Wiley: New York, 1992. (c) Porto, M.; Urbakh, M.; Klafter, J. *Phys. Rev. Lett*. **2000**, *84*, 6058−6061.
(4) Gimzewski, J. K.; Joachim, C. *Science* **1999**, *283*, 1683−1688.
(5) (a) Mekle, R. C. *Nanotechnology* **1991**, *2*, 134−141. (b) Cagin, T.; Jaramillo-Botero, A.; Gao, G.; Goddard, W. A., III. *Nanotechnology* **1998**, *9*, 143−152.
(6) (a) Kinbara, K.; Aida, T. *Chem. Rev*. **2005**, *105*, 1377−1400. (b) For recent reviews on biomolecular machines, see: *Cell* (special issue on macromolecular machines) **1998**, *92*, 291−390.
(7) (a) For the examples of artificial molecular devices and machines, see: *Acc. Chem. Res*. (molecular machines special issue) **2001**, *34*, 409−552. (b) Balzani, V.; Credi, A.; Raymo, F. M.; Stoddart, J. F. *Angew. Chem., Int. Ed*. **2000**, *39*, 3348−3391. (c) Balzani, V.; Credi, A.; Venturi, M. *Molecular Devices and Machines—A Journey into the Nano World*; Wiley-VCH: Weinheim, Germany, 2004. (d) *Molecular Switches*; Feringa, B. E., Ed.; Wiley-VCH: Weinheim, Germany, 2001. (e) Kottas, G. S.; Clarke, L. I.; Horinek, D.; Michl, J. *Chem. Rev*. **2005**, *105*, 1281−1376. (f) Ozin, A. G.; Manners, I.; Fournier-Bidoz, S.; Arsenault, A. *Adv. Mater*. **2005**, *17*, 3011−3018.
(8) Rosei, F.; Schunack, M.; Naitoh, Y.; Jiang, P.; Gourdon, A.; Laegsgaard, E.; Stensgaard, I.; Joachim, C.; Besenbacher, F. *Prog. Surf. Sci*. **2003**, *71*, 95−146.

10.1021/ja058514r CCC: $33.50

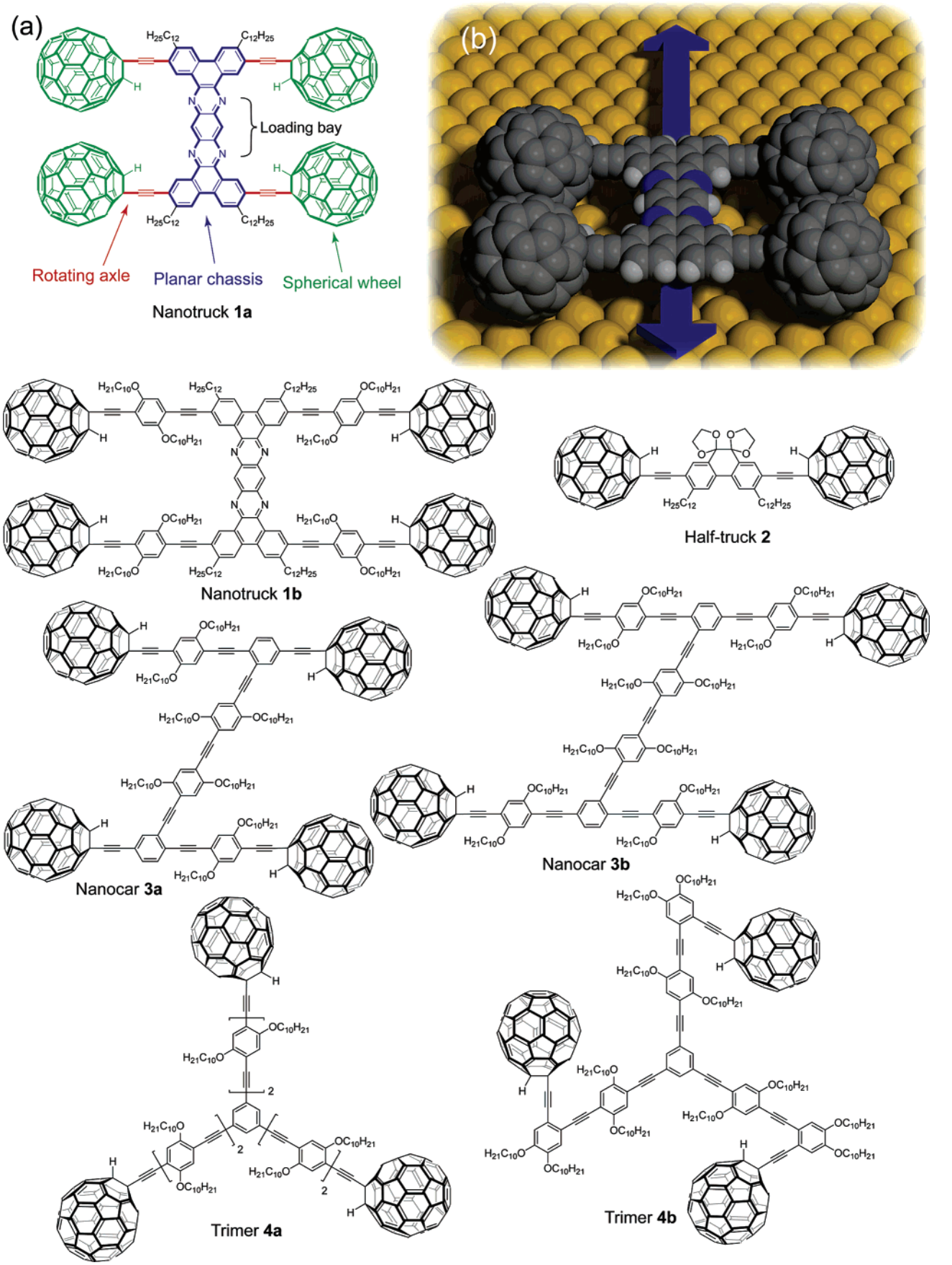

Figure 1. The structures of the fullerene-wheeled molecular machines developed in the present study. (a) Molecular structures of the molecular machines. (b) Space-filling model of the nanotruck **1a** (devoid of dodecyl groups for clarity) on a surface. The blue arrow beneath the molecule illustrates the expected direction of fullerene-wheel-assisted rolling motion.

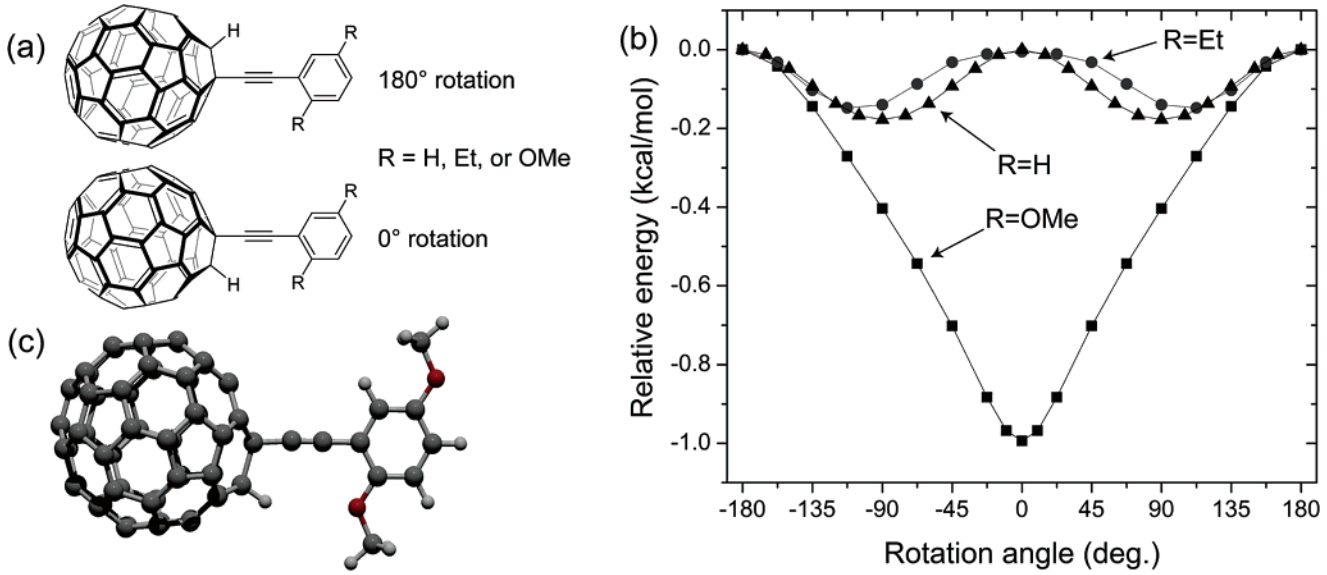

Figure 2. Rotational barrier of the fullerene-wheel structures. Using HF/3-21G level of theory on the (a) fullerene-wheel model compounds with three different substituents, (b) relaxed potential energy surface scans around the wheel rotation were performed (the least stable conformation of each model was set to 0 kcal/mol). (c) Optimized structure of the fullerene-wheel model (R = OMe) at 0° rotation angle.

the entities of comparison; if there were no dissimilarities, the two entities would no longer be analogous. The highest-level formal definition of a vehicle is "any device on wheels for transporting people or objects".[9] We demonstrate here a nanosized "device on wheels for transporting" itself (ca. 100 nm, as recorded), and on that basis, we use the term "nanocar", albeit obviously displayed with dissimilarities from the common macroscopic objects. Likewise, a truck is a "vehicle for hauling loads",[9] and when we constructed a nanosized "device on wheels" that has a platform that might accommodate a load, we used the term "nanotruck".

As shown in Figure 1a, the designed nanotrucks and nanocars consist of three basic molecular mechanical parts: fullerene wheels, a chassis made of fused aromatic rings or oligo(phenylene ethynylene)s (OPEs), and alkynyl axles. The nanotrucks **1a** and **1b** have a potential loading bay (acid−base bonding to the nitrogen atoms), unlike the nanocars **3a** and **3b**. The new synthesis methodology, in situ ethynylation of fullerenes,[10] was developed in order to synthesize these molecular machines. Through the syntheses of several related molecular structure versions, it was clear that the alkyl units were critical for the requisite solubility of these multi-fullerene structures. These highly flexible groups have minimal interactions with surfaces, compared to the strong charge-transfer interaction of the fullerene wheel on gold.[11] The molecule−surface interaction is likely to be dominated by the characteristics specific to the fullerene wheels on gold surfaces; the alkyl groups contribute comparatively little to the surface stiction.

We have successfully demonstrated that our nanomachines exhibit fullerene-wheel-assisted rolling translation and rotation on gold surfaces because of the spherical fullerene wheels connected to a chassis via freely rotating alkynyl axles.[12] The observed rolling motion resembles that of macroscopic cars, and this is the first observation of a molecular-sized machine that incorporates mechanical components, such as wheels and axles, with movement at the single molecule level. While the thrust to design single-molecule-sized nanoscale machines with controlled mechanical motion has yielded a variety of molecular machinery resembling macroscopic motors, switches, shuttles, turnstiles, gears, bearings, and elevators,[7,13] these nanomachines have been operated and observed only spectroscopically as ensembles of molecules in the solution or the solid[13a] state. Examples in which a molecule has a mechanical design and the mechanism of movement can be probed at the single molecular level are limited and include cyclodextrin necklaces,[14] altitudinal molecular rotors,[15] molecular barrows,[16] molecular landers,[17] and nanowalkers.[18]

Results and Discussion

Modeling of Fullerene-Wheeled Nanostructures. One of several promising molecular architectures explored in our group for the synthesis of the surface-capable molecular structures is based on the fullerene wheel and alkynyl axle. We expected that the symmetrical spherical structure of C_{60} would allow the smooth rotation of the molecular wheel. Free rotation of the

(9) *Webster's New Twentieth Century Dictionary*, 2nd ed.; Collins & World: United States, 1975.
(10) Shirai, Y.; Zhao, Y.; Cheng, L.; Tour, J. M. *Org. Lett.* **2004**, *6*, 2129−2132.
(11) (a) Chase, S. J.; Bacsa, W. S.; Mitch, M. G.; Pilione, L. J.; Lannin, J. S. *Phys. Rev. B* **1992**, *46*, 7873−7877. (b) Altman, E. I.; Colton, R. J. *Surf. Sci.* **1993**, *295*, 13−33. (c) Tzeng, C.-T.; Lo, W.-S.; Yuh, J.-Y.; Chu, R.-Y.; Tsuei, K.-D. *Phys. Rev. B* **2000**, *61*, 2263−2272.
(12) Shirai, Y.; Osgood, A. J.; Zhao, Y.; Kelly, K. F.; Tour, J. M. *Nano Lett.* **2005**, *5*, 2330−2334.
(13) (a) Garcia-Garibay, M. A. *Proc. Natl. Acad. Sci. U.S.A.* **2005**, *102*, 10771−10776. (b) Badjiæ, J. D.; Balzani, V.; Credi, A.; Silvi, S.; Stoddart, J. F. *Science* **2004**, *303*, 1845−1849. (c) Balzani, V.; Clemente-León, M.; Credi, A.; Ferrer, B.; Venturi, M.; Flood, A. H.; Stoddart, J. F. *Proc. Natl. Acad. Sci. U.S.A.* **2006**, *103*, 1178−1183.
(14) Shigekawa, H.; Miyake, K.; Sumaoka, J.; Harada, A.; Komiyama, M. *J. Am. Chem. Soc.* **2000**, *122*, 5411−5412.
(15) Zheng, X.; Mulcahy, M. E.; Horinek, D.; Galeotti, F.; Magnera, T. F.; Michl, J. *J. Am. Chem. Soc.* **2004**, *126*, 4540−4542.
(16) (a) Joachim, C.; Tang, H.; Moresco, F.; Rapenne, G.; Meyer, G. *Nanotechnology* **2002**, *13*, 330−335. (b) Rapenne, G. *Org. Biomol. Chem.* **2005**, *3*, 1165−1169.
(17) (a) Otero, R.; Hümmelink, F.; Sato, F.; Legoas, S. B.; Thostrup, P.; Laesgaard, E.; Stensgaard, I.; Galvão, D. S.; Besenbacher, F. *Nat. Mater.* **2004**, *3*, 779−782. (b) Rosei, F.; Schunack, M.; Jiang, P.; Gourdon, A.; Legsgaard, E.; Stensgaard, I.; Joachim, C.; Besenbacher, F. *Science* **2002**, *296*, 328−331.
(18) Kwon, K.-Y.; Wong, K. L.; Pawin, G.; Bartels, L.; Stolbov, S.; Rahman, T. S. *Phys. Rev. Lett.* **2005**, *95*, 166101.

Scheme 1. Synthesis of the Prototype: Half-Truck[a]

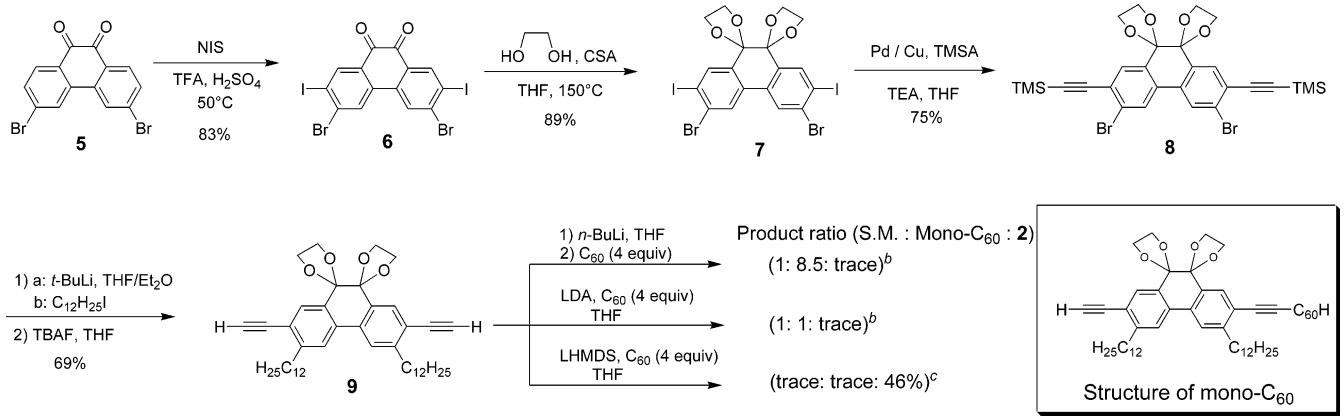

[a] Reagent: Pd/Cu = $PdCl_2(PPh_3)_2$, CuI. [b]Yield determined by ^1H NMR. [c]Isolated yield.

alkynyl axles between the fullerene wheel and chassis should facilitate the rolling motion of the entire molecular vehicle on solid surfaces. To verify this design concept, we have examined the rotational barrier of the wheel and axle architecture using ab initio methods[19] with HF/3-21G level of theory (Figure 2). The result revealed that, even though the phenylene−ethynylene and fullerene π systems have been shown to exhibit an interaction called periconjugation,[20] its contribution to the rotational barrier was expected to be small since the largest estimated barrier height of the three model compounds was only about 1.0 kcal/mol.[21] This low barrier height is actually comparable to that of the triple bond rotation in a usual phenylene−ethynylene system,[22] affording the free rotation of the fullerene-wheel structures at room temperature, or even under cryogenic conditions.

Another key molecular architecture explored in our laboratory for the synthesis of the nanomachines is the chassis design. Working toward the synthesis of fullerene-wheeled nanostructures, we have chosen two different chassis structures: a rigid structure as in nanotrucks **1a** and **1b**, and a semirigid structure as in nanocars **3a** and **3b**. These fullerene-wheeled nanostructures share several features worth mentioning. First of all, most proposed structures weigh more than 4000 Da due to the high molecular weight of each C_{60} (720 Da). Second, integration of as many as four C_{60}s in a well-defined molecular system is rare and not previously known for a rigid molecular system due to the synthetic difficulty associated with fullerene derivatives.[23] This feature made it difficult to obtain highly pure samples of the nanotrucks. The semirigid OPE chassis was introduced to remedy those difficulties met in the rigid chassis system and

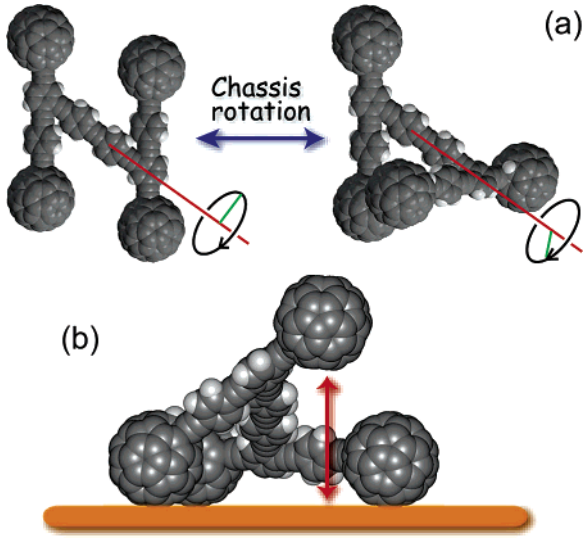

Figure 3. Flexibility of the semirigid chassis structure (nanocar **3a**, devoid of alkoxy groups for clarity). (a) The triple bonds in the OPE structure can rotate until the fullerene wheels touch one another, which gives the nanocar flexibility orthogonal to the surface plane. (b) One fullerene wheel is elevated, while the other wheels remain on the surface to illustrate the suspension concept.

enabled us to perform successful single-molecule STM studies. Better flexibility of OPE structure combined with the increased number of alkyl units dramatically increased the processibility of the massive fullerene-wheeled structures in organic solvents. Furthermore, the rotation around alkyne connections between the chassis and axle portions in the OPE system can cause it to act as suspension, giving the nanocar flexibility orthogonal to the surface plane (Figure 3), and thereby permitting it to climb one-atomic-step high gold islands.[24]

Synthesis Effort toward Multi-Fullerene Structures: Half-Truck Approach. The synthesis of the prototype nanotruck, half-truck **2**, is outlined in Scheme 1. The half-truck **2** was designed and synthesized to develop a reliable synthetic methodology for the attachment of multiple fullerenes to terminal alkynes. The dibromo-diketone **5**[25] was iodinated to give compound **6**. Protection of the diketone moiety of compound **6** was achieved with ethylene glycol.[26] Compound

(19) Frisch, M. J.; et al. *Gaussian 03*, revision C.02; Gaussian, Inc.: Wallingford, CT, 2004 (see Supporting Information for the full author list).
(20) Hamasaki, R.; Ito, M.; Lamrani, M.; Mitsuishi, M.; Miyashita, T.; Yamamoto, Y. *J. Mater. Chem.* **2003**, *13*, 21−26 and references therein.
(21) It appears that the main contribution to this rotational barrier is the very weak interaction between the acidic proton on the fullerene cage and the lone pair electrons on the oxygen atom in the methoxy group because such interaction is missing in the other two model compounds and ethyl and methoxy groups should be similar in terms of sterics. Further confirmation applying B3LYP/6-31G* level of theory to the 0 and 180° rotations of the methoxy model predicted the barrier height to be only 0.54 kcal/mol.
(22) Seminario, J. M.; Zacarias, A. G.; Tour, J. M. *J. Am. Chem. Soc.* **1998**, *120*, 3970−3974.
(23) For well-defined structures with more than four fullerenes attached, see: (a) Nierengarten, J.-F.; Schall, C.; Nicoud, J.-F. *Angew. Chem., Int. Ed.* **1998**, *37*, 1934−1936. (b) Armaroli, N.; Boudon, C.; Felder, D.; Gisselbrecht, J.-P.; Gross, M.; Marconi, G.; Nicoud, J.-F.; Nierengarten, J.-F.; Vicinelli, V. *Angew. Chem., Int. Ed.* **1999**, *38*, 3730−3733. (c) Zhang, S.; Gan, L.; Huang, C.; Lu, M.; Pan, J.; He, X. *J. Org. Chem.* **2002**, *67*, 883−891.
(24) Effect of suspension-like behavior can be possibly observed by STM. Manuscript on the detailed STM study is in preparation by Osgood, A. J.; Shirai, Y.; Zhao, Y.; Kelly, K. F.; Tour, J. M.
(25) Bhatt, M. V. *Tetrahedron* **1964**, *20*, 803−821.

Scheme 2. Synthesis of the Nanotrucks[a]

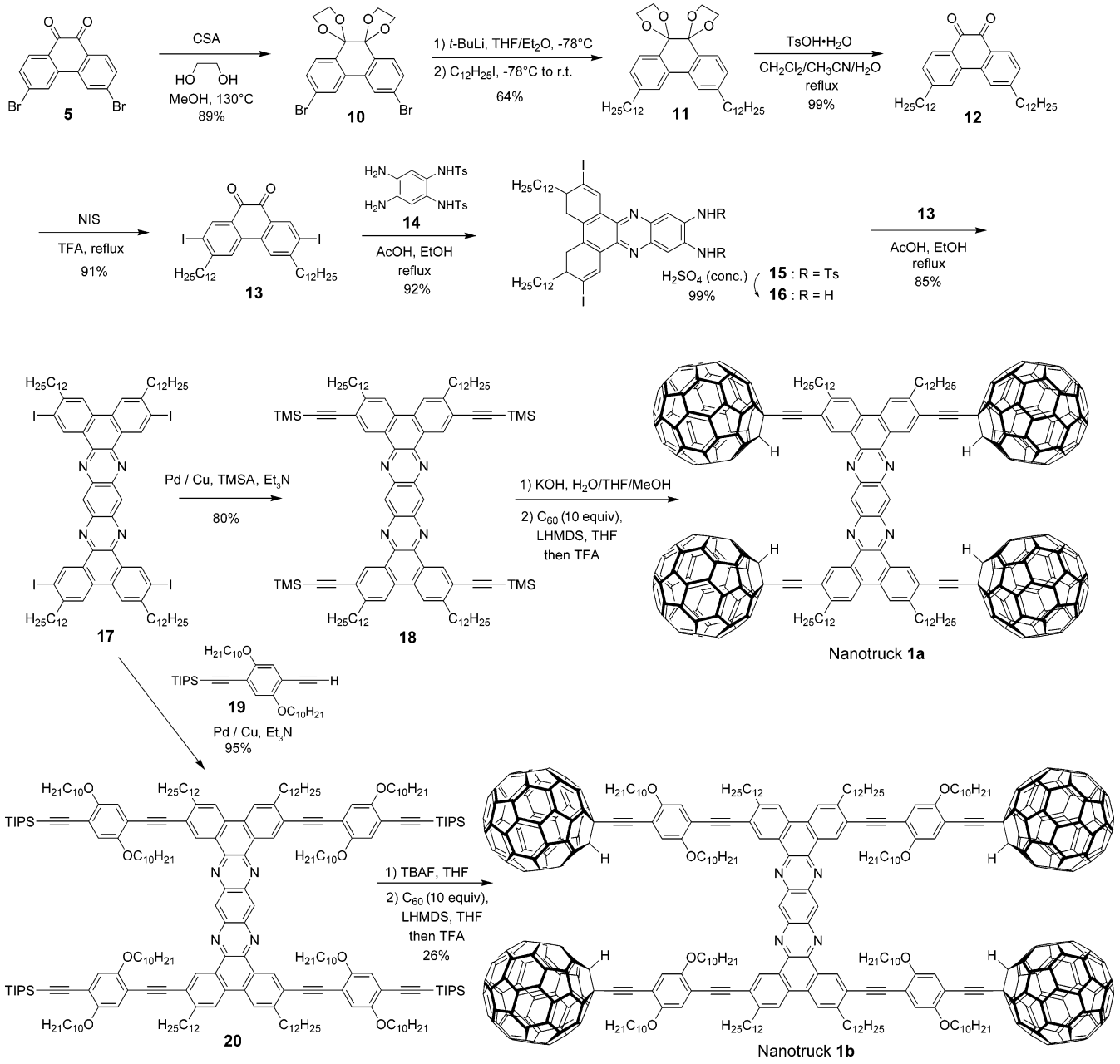

[a] Reagent: Pd/Cu = $PdCl_2(PPh_3)_2$, CuI.

7 underwent a Pd-catalyzed coupling reaction with trimethylsilyl acetylene (TMSA) to give compound **8**. After the lithium−halogen exchange on the bromide followed by quenching with *n*-dodecyl iodide, the TMS protecting group was removed using tetrabutylammonium fluoride (TBAF) in THF to obtain compound **9** in 69% yield over two reaction steps. The key reaction step was achieved in 46% yield after testing numerous different conditions. The breakthrough was afforded when the terminal alkynes were deprotonated in THF using excess LHMDS in the presence of excess C_{60}. Deviation from any one of the conditions dramatically affected reaction outcomes as listed in Scheme 1. This in situ approach was applicable to other substrates and resulted in the preparation of a wide variety of multi-fullerene structures in our laboratory.[27] Indeed, this methodology was so effective that the attachment of as many as four C_{60}s was achieved on the nanocars and nanotrucks. Eventually, all our nanotrucks and nanocars were synthesized by applying this methodology to the tetra-terminal alkyne precursors, as shown in Schemes 2 and 3.

Synthesis and Spectral Characterization of Nanotrucks. The syntheses of nanotrucks **1a** and **1b** are outlined in Scheme

(26) The formation of two fused 1,4-dioxane structures (below) could not be spectroscopically ruled out; however, since deprotection was imminent, no further effort was given to the determination.

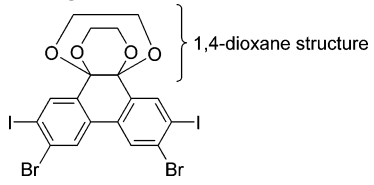

(27) Zhao, Y.; Shirai, Y.; Slepkov, A. D.; Cheng, L.; Alemany, L. B.; Sasaki, T.; Hegmann, F. A.; Tour, J. M. *Chem.—Eur. J.* **2005**, *11*, 3643−3658.

Scheme 3. Synthesis of the Nanocars[a]

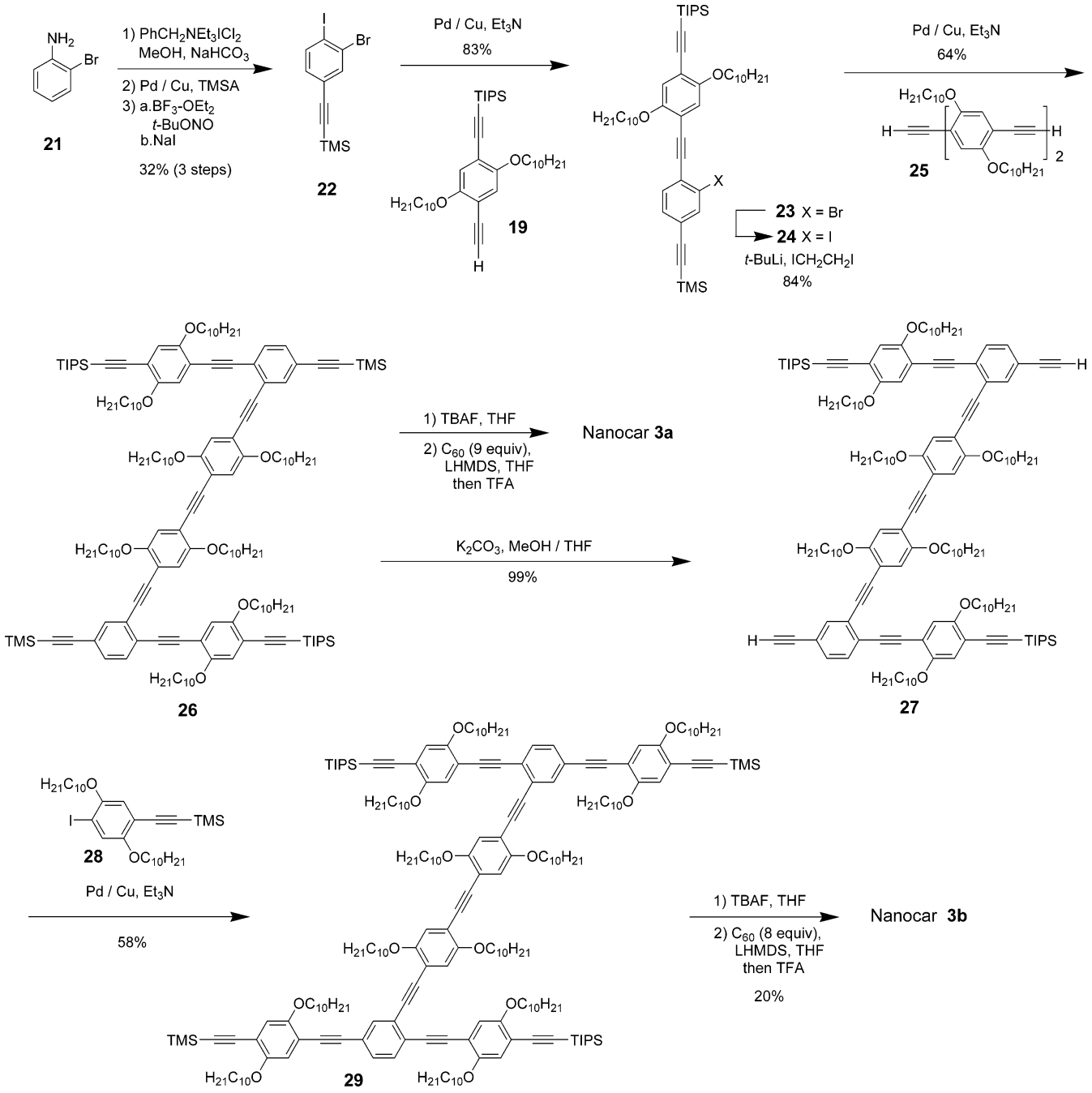

[a] Reagent: Pd/Cu = $PdCl_2(PPh_3)_2$, CuI.

2. The half-truck **2** or its precursors, **8** and **9**, could not be used in the synthesis of nanotrucks **1a** or **1b** because deprotection of the diketone moiety with various aqueous acids was not possible in the presence of alkynes. Alternatively, protecting **5** with ethylene glycol under CSA catalysis afforded diacetal **10**.[26] Compound **10** underwent lithium−halogen exchange reaction with *t*-BuLi to form a dilithiated species that was directly alkylated by *n*-dodecyl iodide to yield compound **11**. Deprotecting of **11** with TsOH in water afforded diketone **12**. Iodination of **12** with NIS in trifluoroacetic acid (TFA) thus afforded diiodide **13**. Compound **13** was condensed with **14** (prepared by bistosylation of 1,2-phenylenediamine, 4,5-dinitration with HNO_3, and finally reduction with Sn/HCl)[28] to afford the half-chassis **15**.[29] Compound **15** was deprotected with H_2SO_4 to give free diamine **16**, which was subsequently condensed with **13** to form the full chassis **17**. Compound **17** was then cross-coupled with TMSA under Pd catalysis to afford the chassis−axle component **18**. Desilylation of **18** with KOH, followed by the in situ ethynylation in THF with excess C_{60} using LHMDS, yielded nanotruck **1a**. As mentioned earlier, the use of excess LHMDS and C_{60} in THF is essential for the successful reaction. Unfortunately, nanotruck **1a** was insoluble in all organic solvents, which prevented us from determining the yield of a pure sample.

(28) Starnes, S. D.; Arungundram, S.; Saunders: C. H. *Tetrahedron Lett*. **2002**, *43*, 7785−7788 and references therein.
(29) Hedberg, F. L.; Arnold, F. E.; Kovar, R. F. *J. Polym. Sci., Polym. Chem. Ed*. **1974**, *12*, 1925−1931.

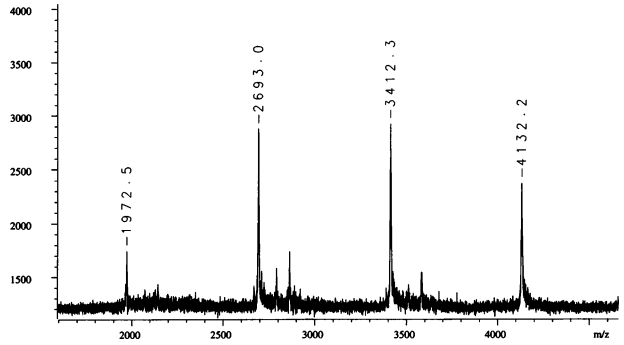

Figure 4. MALDI-TOF mass spectrum of nanotruck **1a**. Peaks for one-, two-, three-, and four-wheel nanotrucks (*m*/*z* 1972.5, 2693.0, 3412.3, and 4132.2, respectively) are observed (negative ion mode, dithranol matrix).

The complete purification of nanotruck **1a** was hampered due to its low solubility in most good organic solvents for fullerene derivatives, such as CS_2 and *o*-dichlorobenzene. Since the fullerene-attached products are the only low solubility components in the reaction mixture, washing the resultant solid from the reaction mixture yielded a brownish solid of **1a**. Although it was impossible to directly determine the purity of the nanotruck **1a** by solution phase NMR or other solution phase techniques, solid state ^{13}C NMR and MALDI-TOF MS analyses can be used to roughly estimate the purity. The formation of nanotruck **1a** was first confirmed by its MALDI-TOF MS spectrum (Figure 4). The molecular ion peak of nanotruck **1a** is clearly observed at *m*/*z* 4132.2, while the signals at *m*/*z* 3412.3, 2693.0, and 1972.5 are assigned to the fragmentations by losing one, two, and three fullerene moieties, respectively, since the peak separations correspond to the mass of C_{60} (720 Da) (Figure 4). In the solid state ^{13}C NMR experiments,[30] aside from the remarkably intense signals for fullerene and chassis aromatic sp^2 carbons at ca. 150−120 ppm, and the *n*-dodecyl carbons at 30.6, 23.6, and 14.4 ppm, distinguishable resonance peaks for the sp^3 carbons on the fullerene core are also observed (Figure 5a). The fullerene C−H carbon was assigned to the resonance at δ 62.1 for several reasons. The signal intensity is significantly increased in the $^1H-^{13}C$ CPMAS experiment (Figure 5b); the signal disappears in a dipolar dephasing experiment,[31] and the chemical shift is consistent with literature data.[27] The quaternary fullerene carbon was assigned to the resonance at δ 55.8 in light of literature data.[27] In Figure 5a, two alkynyl sp carbons are also discernible at δ 83.1 ($C_{60}H-C\equiv C-$) and δ 97.5 ($C_{60}H-C\equiv C-$), respectively, consistent with the solution state ^{13}C NMR data obtained from other multi-fullerene structures.[27]

The proton attached to the fullerene is known to be significantly acidic due to the stabilized aromatic anion structure after its deprotonation,[32] and the chassis contains four nitrogen sites that could possibly be protonated. ^{15}N NMR can clearly differentiate between an imine and an iminium ion (protonation results in a large upfield shift[33]), and thus, we carried out further experiments to shed light on this issue. $^1H-^{15}N$ CPMAS NMR

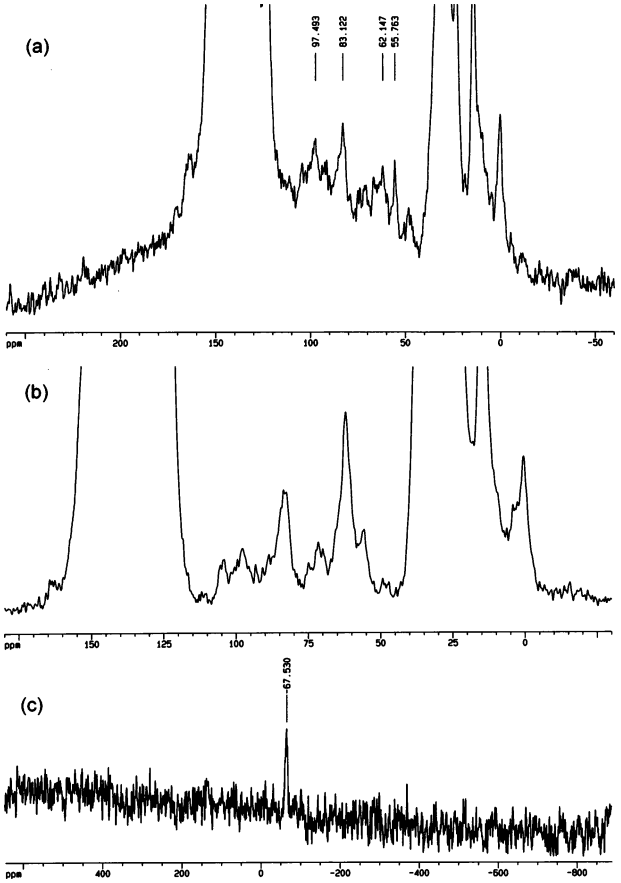

Figure 5. Solid state ^{13}C and ^{15}N NMR spectra of nanotruck **1a**. (a) Direct ^{13}C pulse, MAS at 6.8 kHz. (b) $^1H-^{13}C$ CPMAS, MAS at 6.0 kHz, 3 ms contact time. (c) $^1H-^{15}N$ CPMAS, MAS at 4.0 kHz, 10 ms contact time, relative to glycine defined as 347.58 ppm relative to CH_3NO_2 at 0 ppm.[35]

experiments were conducted on nanotruck **1a** and a model compound dibenzo[*a*,*c*]phenazine that possesses a similar nitrogen moiety. Nanotruck **1a** shows a signal at −67.5 ppm, which is consistent with that of the model compound at −66.7 ppm.[34] Therefore, the analysis indicates that in the solid state the fullerenes in nanotruck **1a** remain neutral rather than in a deprotonated state. Unfortunately, the ^{15}N NMR spectrum could not be improved. Even with a full 7 mm rotor, it took a week of signal averaging (118 000 scans with a 5 s relaxation delay) to acquire this spectrum; with a molecular formula of $C_{330}H_{114}N_4$, nanotruck **1a** contains only 1.4 wt % nitrogen, corresponding to just 0.005 wt % nitrogen-15.

As the four *n*-dodecyl functionalities failed to provide sufficient solubility for nanotruck **1a**, we next tried to alter the axle structure by incorporating compound **19**[10,27] as a solubility enhancer. The tetraiodo full chassis **17** was coupled with **19**, and then fullerene wheels were attached following the same in situ ethynylation procedure to afford the nanotruck **1b** with better solubility. Nanotruck **1b** could be well-purified and fully characterized.

Our next step was aimed at driving the nanotrucks on surfaces in a controllable mode; however, our expectations were not

(30) See Supporting Information for more detail of solid state NMR experiments.
(31) Liang, F.; Alemany, L. B.; Beach, J. M.; Billups, W. E. *J. Am. Chem. Soc.* **2005**, *127*, 13941−13948.
(32) (a) Fagan, P. J.; Krusic, P. J.; Evans, D. H.; Lerke, S. A.; Johnston, E. *J. Am. Chem. Soc.* **1992**, *114*, 9697−9699. (b) Niyazymbetov, M. E.; Evans, D. H.; Lerke, S. A.; Cahill, P. A.; Henderson, C. C. *J. Phys. Chem.* **1994**, *98*, 13093−13098. (c) Timmerman, P.; Anderson, H. L.; Faust, R.; Nierengarten, J. L.; Habicher, T.; Seiler, P.; Diederich, F. *Tetrahedron* **1996**, *52*, 4925−4947. (d) Keshavarz-K, M.; Knight, B.; Srdanov, G.; Wudl, F. *J. Am. Chem. Soc.* **1995**, *117*, 11371−11372. (e) Murata, Y.; Ito, M.; Komatsu, K. *J. Mater. Chem.* **2002**, *12*, 2009−2020.
(33) (a) Botto, R. E.; Roberts, J. D. *J. Org. Chem.* **1979**, *44*, 140−141. (b) Allen, M.; Roberts, J. D. *J. Org. Chem.* **1980**, *45*, 130−135. (c) Muccio, D. D.; Copan, W. G.; Abrahamson, W. W.; Mateescu, G. D. *Org. Magn. Reson.* **1984**, *22*, 121−124.
(34) See Supporting Information for the $^1H-^{15}N$ CPMAS spectrum of the model compound dibenzo[*a*,*c*]phenazine.

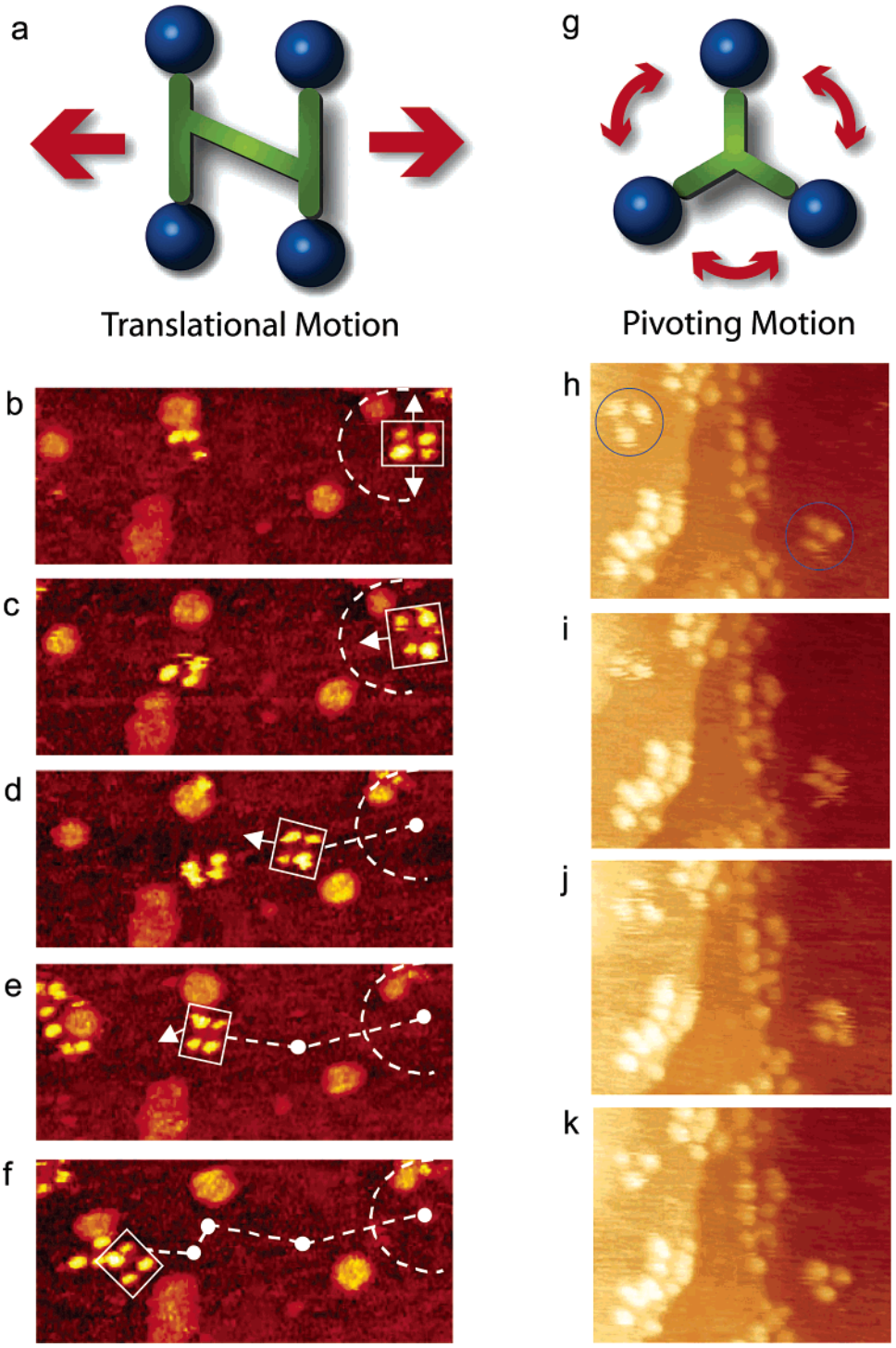

Figure 6. Comparison of thermally induced motions of (a) four-wheeled **3b** and (b−f) its STM-imaged motions, and (g) three-wheeled **4a** and (h−k) its STM-imaged motions. All sequence images were taken during annealing at ~200 °C (bias voltage $V_b = -0.95$ V, tunneling current $I_t = 200$ pA; image size is 51 × 23 nm). The orientation of the nanocar **3b** is easily determined by the fullerene-wheel separation, with motion occurring perpendicular to the axles.[12] Acquisition time for each image is approximately 1 min, with (b−f) selected from a series spanning 10 min, which shows ~80° pivot (b) followed by translation interrupted by small-angle pivot perturbations (c−f). (h−k) A sequence of STM images acquired approximately 1 min apart during annealing at ~225 °C shows the pivoting motion of **4a** (both circled molecules) and lack of translation of any molecules ($V_b = -0.7$ V, $I_t = 200$ pA; image size is 34 × 27 nm). See the Supporting Information for the complete video file and interstitial images.[38]

fulfilled by either of the nanotrucks. Preliminary STM studies on both insoluble **1a** and soluble **1b** nanotrucks revealed rather complicated results. The contamination of the gold surfaces by unreacted fullerenes and possible instability of nanotrucks on gold surfaces inhibited detailed STM studies (vide infra).[36]

Synthesis of Nanocars. Because previously made trifullerene compounds **4a**[10] and **4b**[27] with OPE structure are relatively stable, soluble in common organic solvents, and can be purified free of C_{60}, we combined our fullerene-wheel design with a Z-shaped OPE backbone to produce nanocars **3a** and **3b**

(35) Hayashi, S.; Hayamizu, K. *Bull. Chem. Soc. Jpn.* **1991**, *64*, 688−690.

(36) See Supporting Information for the STM images of nanotrucks **1a** and **1b**.

(Scheme 3). Commercially available compound **21** was iodinated and coupled with TMSA using Pd-catalyzed conditions, and then the amino group was converted to an iodide to afford compound **22**. The subsequent coupling reaction with axle unit **19** gave bromide **23**. After replacing the bromide with iodide using a lithium−halogen exchange reaction, compound **24** was coupled with the middle chassis **25**[10,27] to afford compound **26**. The exchange reaction of the bromide group with iodide was required for a successful coupling reaction with **25**. Surprisingly, our attempts to get pure nanocar **3a** at this stage failed due to the limited solubility of the product. A brown crude solid material was obtained after the removal of solvents; however, it was not soluble enough for further purification and solution phase characterization. To further improve solubility of the nanocar, another solubility enhancing group **28**[10,27] was coupled after chemoselectively removing the TMS protecting groups using K_2CO_3. The coupling reaction with compound **28** yielded full chassis **29**. After the removal of all silyl-protecting groups with TBAF, four fullerene wheels were successfully coupled via the in situ ethynylation method to complete the synthesis of the nanocar **3b**. The nanocar **3b** was an improvement over nanotrucks **1a** and **1b** in terms of stability, solubility, and purity, and it was well-suited for STM studies.

Fullerene-Wheel-Assisted Motion of Nanocars. With nanocar **3b** and three-wheelers **4a** and **4b** (their syntheses being previously described[10,27]), we have been able to demonstrate the action of the fullerene-wheel architecture at the single-molecule level. The evidence for the fullerene-wheel-assisted rolling motion of the nanocars **3b** on the gold surface was obtained by the comparison of two different modes of thermally induced motions: translation and pivoting (Figure 6).

The four-wheeled nanocars **3b** remained relatively stationary on the surface up to approximately 170 °C. As the temperature increased above this point, the molecules began to move in two dimensions through a combination of both translation and pivoting—not in the 1-D manner initially expected.[37] At approximately 200 °C, the motion of the nanocars **3b** is, on average, slow enough to be followed through a series of 1 min images. Pivoting motion can be seen in a sequence of images (Figure 6b−f).[38] The translational motion that occurred between pivoting was perpendicular to the axles, illustrating a directional preference relative to the molecular orientation (the length differing from the width permitted the directional assignment).[12] Above approximately 225 °C, the rapid and erratic motion of the molecules could not be tracked due to the relatively slow acquisition time necessary (approximately 1 min for a 90 × 90 nm scan) compared to the rate of surface diffusion of the molecules.

When three-wheeled nanocars **4** were slowly heated to 225 °C (a higher temperature than needed to induce significant translational motion in the nanocars **3b**), only occasional surface diffusion was observed. Translation in these cases was on the order of only a few nanometers over 20−30 min for those that translated at all. The majority of motion of these molecules was of **4a** pivoting in place around a central pivot point (Figure 6h−k). No significant translation or pivoting motion of trimer **4b** was observed due to the wheel orientation relative to the axles. The pivoting behavior of trimer **4a** continued even up to 300 °C,[39] a temperature at which the four-wheeled nanocars **3b** were moving across the surface too quickly to be imaged by the STM. One would expect the energy barrier for sliding or stick-slip motion for **4a** and **4b** to be comparable or even less than that for **3b** given there is one less fullerene in **4a** and **4b** and thus a weaker overall interaction between the molecule and the gold surface. However, since **4a** and **4b** exhibited little of the thermally induced translation over the temperature range investigated, this further suggests that the motion of nanocar **3b** is due to rolling of the fullerene wheels.[12]

Conclusion

In summary, we have presented the design, syntheses, and testing of new, fullerene-wheeled nanostructures: nanocars and nanotrucks. These single-molecule-sized nanovehicles are composed of three basic nanocomponents that are spherical fullerene wheels, freely rotating alkynyl axles, and a molecular chassis. The use of spherical wheels based on fullerene-C_{60} and freely rotating axles based on alkynes has enabled the directed nanoscale rolling of a molecular structure. The rotational barriers for the fullerene-wheel model compounds, determined by using ab initio methods (HF/3-21G or B3LYP/6-31G* level of theory), confirmed a free rotation of the axle in the designed fullerene-wheel structure. A new synthesis methodology, the in situ ethynylation of fullerenes,[10] was developed for the realization of the fullerene-wheel design. The first generation of our four-fullerene-wheeled nanomachine, nanotruck **1a**, composed of the rigid chassis structure based on fused aromatic rings was not soluble in any solvents we tested. However, its structure was successfully characterized using solid state NMR[30] and MALDI-TOF mass spectroscopy, and preliminary STM imaging was conducted.[36] The second generation, nanotruck **1b**, was soluble due to the incorporation of solubility enhancing axle units and was fully characterized spectroscopically. Detailed STM imaging on these nanotrucks **1** was, however, hampered due to the contamination of surfaces with unreacted fullerenes and possible instability of the nanotruck structures on gold surfaces. In the development of the third generation fullerene-wheeled nanostructure, we incorporated a new chassis design that is based on an OPE structure. The new design contains no nitrogen moieties for cargo purposes and was thus designated as a nanocar. Each monomer unit in the nanocar chassis contains polar decyloxy groups that increase the solubility of the molecule and facilitate the purification process for the removal of unreacted C_{60}. Surprisingly, however, the third generation nanocar **3a** was not soluble. The poor solubility is presumably due to the strong intermolecular interactions caused by the four fullerene wheels. Eventually, after a small modification, the fourth generation nanocar **3b** was synthesized. Nanocar **3b** is soluble, almost completely free from unreacted fullerenes, and suitable for detailed STM studies, which have successfully demonstrated the new type of fullerene-based wheel-like rolling motion, as not being the usual stick-slip or sliding translation. The studies here underscore the ability to control directionality of motion in molecular-sized nanostructures through precise

(37) The observed 2-D motion of the molecules, instead of the expected 1-D motion, can be explained by the ability of the fullerenes to rotate independently of one another, giving rise to a pivoting motion of the molecule on the small atomic corrugation of a Au(111) substrate.

(38) A supplemental movie for this series of images can be found at our website: http//tourserver.rice.edu/movies/.

(39) The onset temperature for decomposition as studied by thermogravimetric analysis on fullerene-wheel model compounds; see Supporting Information.

molecular design and synthesis. Further studies are concentrating on electric field-induced motion of nanocars and nanotrucks and new construction of motorized nanocars integrating a light-powered molecular motor unit as well as nanotrains. Investigation of the new molecular-wheel architectures is also in progress using a variety of spherical molecules, such as carboranes and cyclodextrin−shaft complexes; the inherent insolubility of fullerene-wheeled structures and the necessity to attach fullerenes at the final synthetic step, since they tend to inhibit Pd-catalyzed reactions, makes fullerene wheel replacement welcome.

Experimental Section

General Methods. All reactions were performed under an atmosphere of nitrogen unless stated otherwise. Precursors **5**,[25] **14**,[28] **19**,[10] **25**,[10] and **28**[10] were prepared according to literature procedures (see Supporting Information), and trimers **4a** and **4b** were available from previous studies.[10,27] Reagent grade diethyl ether and tetrahydrofuran (THF) were distilled from sodium benzophenone ketyl. Triethylamine (TEA) was distilled over CaH_2. Fullerene (99.5+% pure) was purchased from MTR Ltd. and used as received. LHMDS (1 M solution in THF) and TBAF (1 M solution in THF) were obtained from Aldrich. Flash column chromatography was performed using 230−400 mesh silica gel from EM Science. Thin layer chromatography was performed using glass plates precoated with silica gel 40 F_{254} purchased from EM Science. Solution state ^1H and ^{13}C NMR spectra were recorded on 400 and 500 MHz spectrometers. Solid state NMR spectra were acquired at 200.13 MHz ^1H, 50.33 MHz ^{13}C, and 20.28 MHz ^{15}N.[30] Melting points were uncorrected. Ultrasonicated fullerene slurry in THF was prepared in general ultrasonic cleaners.

General Procedure for the Coupling of a Terminal Alkyne with an Aryl Halide Using a Palladium-Catalyzed Cross-Coupling (Sonogashira) Protocol. To an oven-dried round-bottom flask equipped with a magnetic stir bar were added the aryl halide, the terminal alkyne, $PdCl_2(PPh_3)_2$ (ca. 2 mol % per aryl halide), and CuI (ca. 4 mol % per aryl halide). A solvent system of TEA and/or THF was added depending on the substrates. Upon completion, the reaction was quenched with a saturated solution of NH_4Cl. The organic layer was then diluted with hexanes, diethyl ether, or CH_2Cl_2 and washed with water or saturated NH_4Cl (1×). The combined aqueous layers were extracted with hexanes, diethyl ether, or CH_2Cl_2 (2×). The combined organic layers were dried over $MgSO_4$, filtered, and the solvent was removed from the filtrate in vacuo to afford the crude product, which was purified by column chromatography (silica gel). Eluents and other slight modifications are described below for each compound.

General Procedure for the Addition of C_{60} to Terminal Alkynes Using LHMDS, In Situ Ethynylation Method. To an oven-dried round-bottom flask equipped with a magnetic stir bar were added the terminal alkyne and C_{60} (2 equiv per terminal alkyne H). After adding THF, the mixture was sonicated for at least 3 h. To the greenish−brown suspension formed after the sonication was added LHMDS dropwise at room temperature over 0.5−1.5 h. As the reaction progressed, the mixture turned into a deep greenish−black solution. During the addition of the LHMDS, small aliquots from the reaction were extracted and quenched with trifluoroacetic acid (TFA), dried, and redissolved in CS_2 for TLC analysis (developed in a mixture of CS_2, CH_2Cl_2, and hexanes). Completion of the reaction was confirmed by the disappearance of the starting materials. The reaction was usually completed within 1.5 h from the beginning of LHMDS addition. Upon completion, the reaction was quenched with TFA to give a brownish slurry. Excess TFA and solvent were then removed in vacuo to afford a crude product that was purified by flash column chromatography (silica gel). Eluents and other slight modifications are described below for each compound.

Nanotruck (1a). To a solution of **18** (0.10 g, 0.065 mmol) in THF (25 mL) were added methanol (2 mL) and a solution of KOH (0.60 g, 11 mmol) in H_2O (2 mL). The mixture was stirred overnight. The suspension was then diluted with $CHCl_3$ and then washed with H_2O (3×). The organic fraction was heated until it became clear, and then dried over $MgSO_4$. After filtration, removal of solvent in vacuo gave desilylated product (71 mg, 87%) as a reddish−orange solid: FTIR (KBr) 3303, 2954, 2923, 2851, 1605, 1467, 1436 cm^{-1}; ^1H NMR ($CDCl_3$, 200 MHz) δ 9.09 (br s, 4H), 8.55 (br s, 2H), 7.83 (br s, 4H), 3.46 (s, 4H), 2.88 (br m, 8H), 1.79 (br m, 8H), 1.50−1.22 (m, 72H), 0.91 (t, J = 6.9 Hz, 12H); meaningful ^{13}C NMR measurement failed due to the limited solubility. The desilylated product (88 mg, 0.070 mmol obtained from multiple desilylation reactions) was subjected to the general in situ ethynylation procedure with C_{60} (504 mg, 0.700 mmol), THF (300 mL), and LHMDS (0.70 mL, 1 M in THF, 0.70 mmol). After adding LHMDS, the mixture was stirred at room temperature for 30 min, then TFA (0.3 mL) was added dropwise. Removal of the solvents in vacuo afforded a black sticky solid, which was rinsed with copious amounts of toluene until the purple color disappeared. Further, sequentially rinsing the solid with MeOH/H_2O (50 mL), chloroform (50 mL), and CS_2 (50 mL) afforded a dark brown solid. The solid was gently ground into fine powder and then sonicated in CS_2 (10 mL) to remove trace amounts of unreacted fullerene. Filtration and drying under vacuum afforded nanotruck **1a** (121 mg, although insolubility precluded adequate purification and yield determination) as a dark brown solid: FTIR (KBr) 2919, 2848, 1682, 1428 cm^{-1}; solid state ^{13}C NMR (50 MHz) δ 160−120 (br), 97.5, 83.1, 62.1, 55.8, 30.6 (br), 23.6, 14.4; solid state $^1H-^{15}N$ CPMAS NMR (20 MHz) δ −67.5; MALDI-TOF MS *m/z* (matrix, dithranol) calcd for $C_{330}H_{114}N_4$ 4134.5, found 4132.2 (M^-).

Nanotruck (1b). To a solution of compound **20** (136 mg, 0.0386 mmol) dissolved in THF (5 mL) was added dropwise TBAF (0.20 mL, 1 M in THF, 0.20 mmol). The solution was stirred at room temperature for 15 min, then the CH_2Cl_2 (20 mL) was added. The solution was washed with 10% HCl, saturated $NaHCO_3$, and brine, then dried with $MgSO_4$. Removal of the solvents under reduced pressure gave the crude desilylated product as a reddish wax. This crude product was subjected to the general in situ ethynylation procedure with C_{60} (277 mg, 0.385 mmol), THF (100 mL), LHMDS (0.38 mL, 1 M in THF, 0.38 mmol), and TFA (0.2 mL). The crude product was purified by a silica column chromatography with a gradient eluent (5:1 hexane/CS_2 to 1:1:1 hexane/CS_2/CH_2Cl_2) to yield the nanotruck **1b** as a dark reddish solid (57 mg, 26%): FTIR (KBr) 2920, 2850, 1634, 1497 cm^{-1}; ^1H NMR ($CDCl_3$/CS_2, 500 MHz) δ 9.67 (br s, 4H), 8.31 (br s, 4H), 7.14 (m, 14H), 4.14 (br m, 16H), 3.24 (br s, 8H), 1.98 (br s, 24H), 1.63 (br s, 24H), 1.50−0.99 (m, 160H), 0.90 (t, J = 6.62 Hz, 12H), 0.83 (t, J = 6.80 Hz, 12H), 0.78 (t, J = 6.72 Hz, 12H); ^{13}C NMR ($CDCl_3$, 125 Hz) δ 154.5, 153.7, 153.6, 151.6 (×2), 151.5, 147.7, 147.6, 147.4, 146.7, 146.5, 146.3, 145.9, 145.8, 145.7, 145.6, 145.5, 145.4, 144.8, 144.6, 144.2, 143.3, 142.7 (×2), 142.2, 142.1, 142.0, 141.4, 140.5, 140.4 (×2), 136.2, 135.2, 132.1, 131.5, 128.8, 123.6, 123.1, 116.6, 115.0, 113.2 (30 signals from sp^2-C in the C_{60} core and 15 signals from sp^2-C in the aromatic ring; 4 signals are missing due to overlapping), 97.7, 94.2, 91.3, 80.8, 69.5, 69.4, 62.1 (*C*H in the C_{60} core), 55.6 (quaternary sp^3-C in the C_{60} core), 35.7, 32.2 (×2), 31.3, 31.2, 30.3, 30.2 (×2), 30.1 (×2), 30.0 (×2), 29.9, 29.8, 29.7 (×2), 27.0, 26.5, 23.1 (×2), 23.0, 14.5, 14.4 (×2); MALDI-TOF MS *m/z* (matrix, dithranol) calcd for $C_{442}H_{290}N_4O_8$ 5785.1, found 5785 (M^+).

Half-Truck (2). Compound **9** (0.068 g, 0.1 mmol) was subjected to the general in situ ethynylation procedure with C_{60} (0.288 g, 0.4 mmol), THF (100 mL), LHMDS (0.8 mL, 1.0 M in THF, 0.8 mmol), and TFA (0.3 mL, 0.39 mmol). Flash column chromatography on silica gel with CS_2:hexane (1:1) (1−2 L) to recover all unreacted C_{60} (0.167 g, 58% of starting material) and with CS_2:CH_2Cl_2:hexane (1:1:3) to collect product afforded the half-truck **2** as shiny brown powder (0.098 g, 46%). Elution with CS_2:CH_2Cl_2:hexane (1:4:5) can recover unreacted compound **9** and mono-C_{60}, if present: FTIR (KBr) 2918, 2848, 1427, 1384, 1187, 1093 cm^{-1}; ^1H NMR (CS_2/$CDCl_3$, 400 MHz) δ 8.18 (s, 2H),

7.92 (s, 2H), 7.18 (s, 2H, C_{60}−H), 4.37 (br s, 4H), 3.84 (br s, 4H), 3.20 (t, J = 8.0 Hz, 4H), 1.98 (q, J = 7.7 Hz, 4H), 1.62−1.23 (m, 36H), 0.87 (m, 6 H); ^{13}C NMR (CS_2/$CDCl_3$, 100 MHz) δ 151.6, 151.5, 147.8, 147.63, 147.57, 146.9, 146.63, 146.61, 146.5 (×2), 146.0, 145.9, 145.77, 145.72, 145.66, 145.58, 144.9, 144.7, 143.4, 142.83, 142.80, 142.34, 142.27, 142.20, 142.1, 141.9, 141.8, 140.7, 140.6, 136.3, 135.3, 133.2, 131.5, 130.9, 124.9, 122.8 (30 signals from sp^2-C in the C_{60} core and 6 signals from sp^2-C in the aromatic ring), 97.1 (C≡C), 92.5, 82.8 (C≡C), 61.9 (*C*H in the C_{60} core), acetal peak was hidden, 55.6 (quaternary sp^3-C in the C_{60} core), 35.9, 32.2, 31.8, 30.6, 30.24, 30.21, 30.1, 30.09, 30.0, 29.7, 23.0, 14.4; MALDI-TOF MS *m*/*z* (matrix, dithranol) calcd for $C_{166}H_{64}O_4$ 2121, found 2121 (M^+).

Nanocar (3a). To a solution of **26** (0.085 g, 0.036 mmol) in THF (15 mL) was added dropwise TBAF (0.3 mL, 0.3 mmol). Ten minutes after the addition of the TBAF, the reaction was quenched with saturated aqueous NH_4Cl and extracted twice with hexanes. The organic portion was dried over $MgSO_4$ and filtered. After concentration in vacuo, the residue was purified by flash column chromatography with 30% CH_2Cl_2 in hexanes to give desilylated product (0.065 g) as a green−yellow solid. Desilylated material (0.060 g, 0.031 mmol) was subjected to the general in situ ethynylation procedure with C_{60} (0.20 g, 0.28 mmol), THF (100 mL), LHMDS (0.6 mL, 0.6 mmol), and TFA (0.3 mL). A brown solid crude material was obtained after the removal of solvents; however, it was not soluble enough for further purifications and solution phase characterizations.

Nanocar (3b). To a solution of **29** (0.096 g, 0.030 mmol) in THF (5 mL) was added dropwise TBAF (0.2 mL, 0.2 mmol). Ten minutes after the addition of the TBAF, the reaction was quenched with saturated aqueous NH_4Cl and extracted twice with hexanes. The organic portion was dried over $MgSO_4$ and filtered. After concentration in vacuo, the residue was purified by flash column chromatography with 30−42% CH_2Cl_2 in hexanes to give desilylated product (0.072 g) as a yellow oil. This material was pure enough to carry on to the next reaction. The desilylated product (0.070 g, 0.025 mmol) was subjected to the general in situ ethynylation procedure with C_{60} (0.15 g, 0.21 mmol), THF (100 mL), LHMDS (0.7 mL, 0.7 mmol), and TFA (0.7 mL). (Note: product spot was not clearly visible on TLC.) Crude products were dissolved in CS_2 and directly loaded onto a column. The column was eluted with CS_2/CH_2Cl_2 (100:1) to remove unreacted C_{60}, and then with CS_2/CH_2Cl_2 (1:1) for complete removal of trace C_{60} and elution of product. The product was further purified using another flash column with graduate elution of CS_2/CH_2Cl_2/hexanes (1:1:100), (3:2:5), then (3:3:4) to afford nanocar **3b** (0.028 g, 20%) as a brown solid: FTIR (CH_2Cl_2 cast) 2922, 2850, 2203, 1502, 1463, 1214 cm^{-1}; ^{1}H NMR (500 MHz, $CDCl_3$) δ 7.77 (d, J = 1.4 Hz, 2H), 7.58 (d, J = 8.0 Hz, 2H), 7.51 (dd, J = 8.0, 1.4 Hz, 2H), 7.30 (s, 2H), 7.25 (s, 2H), 7.18 (s, 2H), 7.15 (s, 2H), 7.14 (s, 2H), 7.10 (s, 2H), 7.07 (s, 2H), 7.03 (s, 2H), 4.19−4.14 (m, 8H), 4.09 (m, 4H), 4.00 (m, 4H), 3.90−3.88 (m, 8H), 1.95−1.13 (m, 192H), 0.88−0.80 (m, 36H); ^{13}C NMR (125 MHz, $CDCl_3$) δ 154.7, 154.6, 153.9, 153.75, 153.67, 153.65, (6 signals from aryloxy sp^2-C in the aromatic ring), 151.65, 151.59, 151.497 (×2), 147.7 (×2), 147.44, 147.43, 146.74, 146.69, 146.50, 146.477 (×2), 146.46, 146.32 (×2), 146.31 (×2), 145.92, 145.89, 145.82, 145.77, 145.72, 145.69, 145.55, 145.529 (×2), 145.51, 145.45, 145.43, 144.78, 144.76, 144.60, 144.58, 143.28, 143.26, 142.69, 142.67, 142.66, 142.64, 142.21, 142.17, 142.13, 142.11, 142.07, 142.05, 141.98, 141.95, 141.77, 141.73, 141.69, 141.67, 140.47, 140.44, 140.40, 140.37, 136.18, 136.15, 135.3, 135.2 (30 × 2 signals from sp^2-C in the C_{60} core), 134.4, 131.6, 130.9, 126.5, 125.8, 123.3, 117.6, 117.4 (×2), 117.2, 117.0, 116.9, 114.9, 114.7, 114.4, 114.2, 113.4, 113.2, 97.8, 96.1, 94.3, 94.1, 93.1, 92.2, 91.8, 91.0, 88.3, 80.2 (×2), 70.14, 70.10, 69.8, 69.6, 69.5, 69.3, 62.02, 61.98 (*C*H in the C_{60} core), 55.60, 55.59 (quaternary sp^3-C in the C_{60} core), 32.04, 31.97, 31.95, 29.8, 29.74, 29.70, 29.66, 29.48, 29.45, 29.40, 22.77, 22.75, 22.73, 14.23, 14.21, 14.19; MALDI-TOF MS *m*/*z* (sulfur as the matrix) calcd for $C_{430}H_{274}O_{12}$ 5632, found 5631 (M^+).

Sample Preparation and Data Collection for STM Study. The nanotrucks **1a** and **1b** were solution spin-coated in air on hydrogen-flame-annealed gold on mica surfaces and then imaged under ambient conditions and then in ultrahigh vacuum. Even in vacuum, these samples appeared to rapidly degrade upon scanning. This might be due to the electrophilicity of the nanotruck cores or to impurities introduced from the deposition protocol. With this limited success, the design of the molecule was changed to that of the nanocars. Following preliminary investigation of the nanocar molecules, our apparatus was modified to allow dosing of the molecules directly from solvent into vacuum onto freshly sputtered and annealed gold on mica. A majority of the nanocar data discussed in this work were obtained with this new sample deposition technique. Given this new deposition method, it might be possible to return to the nanotrucks and obtain better images of their motion. However, owing to the increased ease of synthesis and improved solubility of the nanocars over the nanotrucks, we focused subsequent imaging efforts exclusively on the nanocars. Hence, nanocar **3b** was initially suspended in toluene (5 μM) and initially spun-cast on Au(111) on mica and imaged in an ambient, home-built STM. Following that initial investigation in air, the toluene solution of **3b** was dosed in high vacuum using a fast-actuating, small orifice solenoid valve[40,41] onto argon-sputtered and annealed Au(111) on mica substrates and was imaged using an RHK variable temperature UHV−STM. The dosing technique was chosen over sublimation in vacuum, as it appeared in thermal decomposition studies using a thermogravimetric analyzer on related OPE−alkynyl−fullerenes that the fullerene-based wheels began to cleave from the alkynyl axles at ca. 300 °C with rapid decomposition occurring by 350 °C.[39] A piece of silicon, placed directly underneath the gold substrate, was resistively heated to perform variable temperature studies in the STM. The sample temperature was measured by a K-type thermocouple wire placed directly on the gold surface.

Acknowledgment. The Welch Foundation, Zyvex Corporation, and the NSF Penn State MRSEC funded this work. The Office of Naval Research funded the 200 MHz NMR spectrometer, and the National Science Foundation provided partial funding of the 400 and 500 MHz NMR spectrometers. We thank Drs. I. Chester of FAR Research Inc. and R. Awartani of Petra Research Inc. for providing TMSA, Tomi Hashizume and Yasuhiko Terada for their expertise in vacuum deposition with the solenoid pulse valve, and Paul Weiss for his insight concerning the STM investigations of these molecules.

Supporting Information Available: NMR spectra of all new compounds, TGA spectra of model fullerene-wheel compounds, ^{1}H−^{15}N CPMAS spectra of model compound dibenzo[*a*,*c*]-phenazine, detailed syntheses of the intermediate compounds, and preliminary STM images of nanotrucks **1a** and **1b** are available. Movie files for nanocar **3a** and trimers **4** are available at http://tourserver.rice.edu/movies/. This material is available free of charge via the Internet at http://pubs.acs.org.

JA058514R

(40) Kanno, T.; Tanaka, H.; Nakamura, T.; Tabata, H.; Kawai, T. *Jpn. J. Appl. Phys.* **1999**, *38*, L606−607.
(41) Terada, Y.; Choi, B. K.; Heike, S.; Fujimori, M.; Hashizume, T. *Nano Lett.* **2003**, *3*, 527−531.